Anthropogenic climate change drives shift and shuffle in North Atlantic phytoplankton communities

Andrew D. Barton[a,1], Andrew J. Irwin[b], Zoe V. Finkel[c], and Charles A. Stock[a]

[a]Geophysical Fluid Dynamics Laboratory, National Oceanic and Atmospheric Administration, Princeton University, Princeton, NJ 08540; [b]Department of Mathematics and Computer Science, Mount Allison University, Sackville, NB, Canada, E4L 1A7; and [c]Environmental Science Program, Mount Allison University, Sackville, NB, Canada, E4L 1A7

Anthropogenic climate change has shifted the biogeography and phenology of many terrestrial and marine species. Marine phytoplankton communities appear sensitive to climate change, yet understanding of how individual species may respond to anthropogenic climate change remains limited. Here, using historical environmental and phytoplankton observations, we characterize the realized ecological niches for 87 North Atlantic diatom and dinoflagellate taxa and project changes in species biogeography between mean historical (1951–2000) and future (2051–2100) ocean conditions. We find that the central positions of the core range of 74% of taxa shift poleward at a median rate of 12.9 km per decade (km·dec^{-1}), and 90% of taxa shift eastward at a median rate of 42.7 km·dec^{-1}. The poleward shift is faster than previously reported for marine taxa, and the predominance of longitudinal shifts is driven by dynamic changes in multiple environmental drivers, rather than a strictly poleward, temperature-driven redistribution of ocean habitats. A century of climate change significantly shuffles community composition by a basin-wide median value of 16%, compared with seasonal variations of 46%. The North Atlantic phytoplankton community appears poised for marked shift and shuffle, which may have broad effects on food webs and biogeochemical cycles.

phytoplankton | climate change | North Atlantic | diatom | dinoflagellate

Earth system models (ESMs) generally indicate that greenhouse gas emissions may, over the coming century, lead to further acidification and warming of the ocean surface, increased surface stratification and decreased mixing depths, and weaker seasonal entrainment of deep nutrients essential for phytoplankton growth (1, 2). These global trends are seen in the North Atlantic, although regional variations are apparent (Fig. S1). Many models project that waters southeast of Greenland will become cooler, more stratified, and consequently nutrient-poor (1–3). Here, strong salinity-driven surface stratification arising from ice melt and enhanced precipitation over evaporation may weaken meridional overturning (4). The cooling here is associated with weaker transport of heat into the surface laterally and from below by convection but is also because stratified surface waters are exposed to the relatively cold atmosphere for a longer duration (5). Projected basin-scale changes in clouds and sea ice cover may also drive changes in light entering the ocean surface.

These environmental changes may lead to pronounced regional changes in phytoplankton communities, overlying a global trend of decreasing primary production, weaker sinking flux of particulate carbon, and decreased energy flows between phytoplankton and fish (1, 2, 6). Although it is widely believed that marine organisms and ecosystems are sensitive to climate change (7–11), the climate response and drivers of change for individual phytoplankton species are not well known. The goal of this study is to estimate how anthropogenic climate change in the coming century may alter the biogeographies of many phytoplankton species commonly sampled in the subpolar and subtropical North Atlantic, a region projected to have pronounced regional climate changes and with importance to global biogeochemical cycles and fisheries.

We used the bioclimate envelope approach (12), in which we quantified the realized ecological niche for each species from

historical observations and applied this species distribution model (SDM) to map and compare species biogeographies in modeled historical (1951–2000) and projected future (2051–2100) ocean conditions (Methods and Supporting Information). The SDM for each species was constructed with the MaxEnt modeling method (13–17) by pairing 60 y of Continuous Plankton Recorder (CPR; SI Text) (18) presence-only data with repeating annual cycles for observed environmental predictor variables generally found to affect phytoplankton abundance and community composition: sea surface temperature (SST); sea surface salinity (SSS); mixed layer depth (MLD); photosynthetically active radiation (PAR); and the surface concentrations of nitrate, phosphate, and silicate. We used species abundance data for 1947–2006 in 41 standard survey areas across the North Atlantic (19) and converted abundance to presence-only data because it is difficult to confirm the absence of rare species present in low concentrations. Data for the seven environmental drivers were spatially averaged to match the CPR data. To make biogeographic projections for modeled historical and future periods, data for the same seven environmental predictors were taken from the Geophysical Fluid Dynamics Laboratory's Earth System Model (20, 21) (GFDL ESM2G, 1° horizontal resolution; SI Text), forced by the Representative Concentration Pathway 8.5 (RCP8.5) emissions scenario (Fig. S1). We present results only for a relatively robust set of CPR taxa having greater than 15 presence observations (22) and comparatively high SDM skill, defined here as having an area under the receiver operating characteristic curve (AUC) greater than 0.7 (Supporting Information). We then performed a visual inspection of predicted ranges against CPR presence observations on a season by season basis to assess the robustness of these thresholds (Fig. S2). The resulting 87 taxa (Table S1) represent a diverse subset of commonly sampled North Atlantic diatoms and dinoflagellates, which are

important, but by no means the only, constituents in regional food webs (23, 24) and biogeochemical cycles (25).

Our approach leverages extensive observations to provide an estimate of the direction and magnitude of biogeographic and community compositional changes for North Atlantic diatoms and dinoflagellates but has inherent limitations. A consequence of using presence-only data is that rare and common species living in the same conditions will have the same modeled probability of occurrence. Thus, we focus on changes in biogeography rather than species abundance or biomass, consistent with the limitations of the CPR data and strengths of MaxEnt. Our approach also assumes that microevolutionary change is slow and dispersal is fast relative to the timescales of climate change and that the realized niche with respect to the predictor variables considered remains constant. The SDMs are fixed with respect to long-term trends in abundance, invasions of new species or functional groups into the region, or evolutionary changes in niches, all of which are possible with long-term anthropogenic climate change (26, 27).

Results and Discussion

We find, in common with previous studies (28), that North Atlantic phytoplankton taxa exhibit characteristic biogeographies, reflective of organism traits and biological interactions as they map onto contrasting ocean habitats (9, 13, 29). In the historical period, for example, *Bacteriastrum* spp., a genus of relatively small, chain-forming diatoms, is most likely to be found in subtropical and temperate regions; *Ceratium arcticum*, a large and possibly mixotrophic dinoflagellate, is most common in the northwest Atlantic; and *Rhizosolenia stolterfothii*, an intermediately sized, chain-forming diatom, is most conspicuous in the intergyre transition region (Fig. 1*A*).

As the climate changes over the coming century, the range of each taxon shifts in space. For example, *Bacteriastrum* spp. become more common in the subpolar gyre and less common in the subtropics (Fig. 1 *B* and *C*). The central position of the core range (*Methods*) for 74% of taxa shifts northward and for 26% shifts southward, with a median northward displacement of 12.9 km per decade (km·dec⁻¹) [interquartile range (IQR) −2.07–28.5 km·dec⁻¹;

Fig. 2 *A* and *B*]. Ninety percent of species shift eastward, and 10% shift westward, with a median eastward displacement of 42.7 km·dec⁻¹ (IQR 12.1–68.3 km·dec⁻¹). The preponderance of northward range shifts is consistent with the projected poleward displacement of isotherms and nutrient regimes (8, 9), but the relatively large longitudinal shifts in the North Atlantic are driven by the pronounced regional redistribution of ocean circulation and surface conditions (Fig. S1). Similar longitudinal redistributions of North Atlantic plankton communities in response to changing climate are a common feature in other modeling studies, although the degree of these changes varies across models (2, 30). The projected weakening of the overturning circulation is associated with a central subpolar gyre habitat with weaker mixing, lower nutrients, and cooler temperatures. This habitat has no modern analog in the North Atlantic, and accordingly, many species ranges move eastward and away from this region. These regional changes may also explain why a number of subpolar taxa exhibit a surprising southeastward range shift (Fig. 2*A*). For taxa normally found in the subpolar gyre where overturning weakens, this region may become too stratified and nutrient poor, causing their range to move to the east. It is also possible that cold-adapted taxa may find a temperature refuge in cooler waters of the central subpolar North Atlantic.

Previous modeling studies have found that diatoms, which are generally more common in colder, nutrient-rich systems (13, 31, 32), may become scarcer or retreat northward in a warming climate (30, 33), whereas the fate of dinoflagellates remains largely unknown. Of the taxa we considered, 65% of diatoms exhibit a northward shift, largely consistent with expectations. Eighty-five percent of dinoflagellates also exhibit northward biogeographic shifts, and the median northward shift for dinoflagellates (20.9 km·dec⁻¹, IQR 6.73–30.4 km·dec⁻¹) exceeds that of diatoms (8.50 km·dec⁻¹, IQR -7.21–25.0 km·dec⁻¹; Fig. S3). Species with more southerly historic ranges, many of which are dinoflagellates, are likelier to shift northward than species with more northerly historic ranges (Fig. 2*A*). Dinoflagellates are more often found in warmer, more stratified waters with lower nutrients and turbulence (13, 31, 32), and climate change may
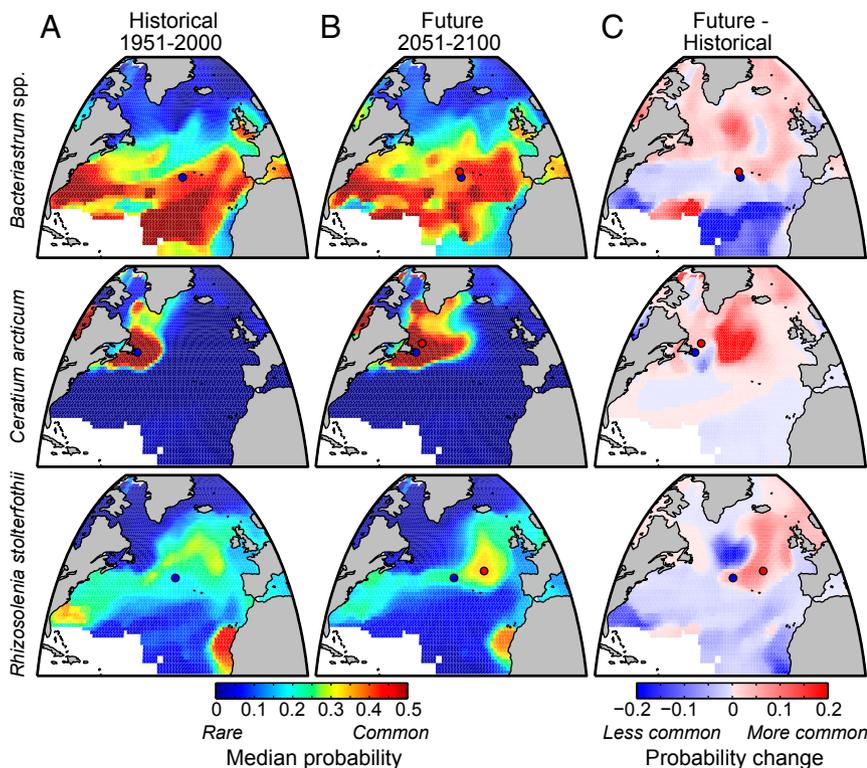
Fig. 1. Estimated biogeographies for *Bacteriastrum* spp. (diatom), *Ceratium arcticum* (syn. *Neoceratium arcticum*; dinoflagellate), and *Rhizosolenia stolterfothii* (syn. *Guinardia striata*; diatom) in 1951–2000 (*A*) and 2051–2100 (*B*) and the change in probability of occurrence (2051–2100 − 1951–2000) (*C*). Map colors in *A* and *B* indicate annual median probability of occurrence, and colors in *C* indicate difference in annual median probability of occurrence; white areas are outside range of environmental training data. The annual median core range central positions in historic (blue dot) and future (red dot) periods are shown for each species. The difference in position between red and blue dots corresponds to the change vectors in Fig. 2. Display data here and in following figures have been smoothed with a 5° × 5° median filter.

Fig. 2. The central position change in core biogeographical range from 1951–2000 to 2051–2100 for each taxon is shown in *A* and projected with equivalent starting positions in *B*. The starting latitude and longitude position in *A* for each taxa is the median latitude and longitude position over the year, and the change vector is the median change in central position over the year. Red (blue) arrows indicate northward (southward) range shifts. Community similarity, as measured by Bray–Curtis similarity index (*Methods*), between a subpolar location (white dot; 57°N, 43°E) in 1951–2000 and adjacent communities in 1951–2000 (*C*) and 2051–2100 (*D*). *E* and *F* show similar sequence for a subtropical location (32°N, 54°E). The solid black contour indicates communities that are 90% similar to communities at each white dot in 1951–2000, and the black dotted contour shows communities that are 90% similar in 2051–2100.

consequently allow their ranges to expand northward in the North Atlantic. However, our results indicate a wide range of climate responses among diatom and dinoflagellate taxa, reflecting the great diversity of cell sizes, functional traits, and predator–prey interactions represented within each functional group (34, 35).

Overall, the poleward shifts in range central positions found in this study (12.9 km·dec^{-1}) are larger than previously estimated for marine taxa within the recent observational record (36) (2.3 km·dec^{-1}) and reflect the large anticipated environmental changes over the coming century relative to observed historical changes. Although not estimated here, changes in the poleward, leading range edge through time may be even more dynamic than the central position calculated here (36).

As species ranges shift, so do entire communities. We mapped the Bray–Curtis similarity index (*Methods*), from 1 for completely similar to 0 for completely different communities, between the historical community at a reference point in the subpolar gyre (white dot) and all other locations in the study area, first for the historical period (Fig. 2*C*) and then for the future (Fig. 2*D*). The phytoplankton community in the central

subpolar gyre is most similar to nearby locations but shifts northeastward and away from the Canadian maritime region during the future period (Fig. 2 *C* and *D*). The community characteristic of the central subtropical gyre, indicated by the white dot in Fig. 2 *E* and *F*, expands northward and onto continental shelves of the Iberian Peninsula in the future period. However, the broad division between subtropical and subpolar habitats largely persists (indicated by contrasting regions with similar communities in Fig. 2 *C* and *D* and Fig. 2 *E* and *F*, respectively) because this is maintained by prevailing and relatively stable patterns of atmospheric and oceanic gyre circulation. Thus, the spatial shifts of species and communities are significant but generally contained within strongly contrasting ocean gyre habitats.

Communities are also projected to internally reorganize, or shuffle. Across the basin, there is considerable change in community composition from the historical to future periods (Fig. 3*A*), with a basin-wide median change in community composition of 16% (*Methods*). This climate shuffle is considerable, although generally smaller than the 46% seasonal change in community composition in the historical period (Fig. 3*B*; within the future period, the seasonal change is also 46%). The relatively large magnitude of seasonal changes is not surprising, because pronounced seasonal changes in the North Atlantic oceanic conditions drive a large spring bloom and strong seasonal succession. However, there are regions in the central North Atlantic and Norwegian Sea where the community climate response may be quite large and of similar magnitude to historical seasonal changes.

Changes in species richness are possible and contribute to community shuffle. Much as for community similarity (Fig. 3 *A* and *B*), changes in richness over the year within the historical period are larger than expected with climate change. However, there is a general decrease in species richness in the subtropical gyre but an increase in higher latitudes in response to climate change (Fig. 3*C*), consistent with previous estimates (9). Within the diatom and dinoflagellate assemblages (Fig. S4), these broad patterns also hold, with the notable exception that dinoflagellate diversity may decrease south of Greenland in the central subpolar gyre. The diversity increase across all species is strongest in winter in the central North Atlantic (Fig. 3*D*). During summer, species richness is reduced in the subtropical gyre and in the central North Atlantic but increased in the intergyre zone and Norwegian Sea (Fig. 3*E*). The large community changes in the central North Atlantic are coincident with the region of pronounced freshening, decreased mixing, lower nutrients, and cooling that are associated with the projected weakening of meridional overturning circulation. During summer, up to 35% of species present here in historical conditions may become locally extirpated over the coming century (Fig. 3*E*). However, no individual species considered here is extirpated from the entire basin and whole year.

In a further set of experiments, we assessed the relative contribution of climate-driven changes in each environmental driver to future phytoplankton community structure at each location (*Methods*). To do so, we individually substituted future environmental conditions for each driver and reprojected the biogeography for each species from its SDM to determine the effect of a change in only one variable at a time. We find that the projected shift and shuffle in the North Atlantic are the result of multiple environmental stressors acting in concert, reflecting the pronounced changes in regional oceanography rather than simply a global mean trend toward warmer, more stratified surface ocean conditions (Fig. 4). Changes in MLD and PAR in our model exert the most spatially widespread and relatively large effect on the phytoplankton assemblages. Changes in nitrate and temperature have widespread but relatively small effects, and changes in silicate, salinity, and phosphate have relatively small and/or localized effects. MLD influences the time-integrated light experienced by phytoplankton and the concentration of nutrients and grazers. This multifaceted influence, together with projected regional MLD changes (Fig. S1), contributes to the

Fig. 3. Bray–Curtis similarity index comparing annual median probability between future (2051–2100) and historical (1951–2000) periods (*A*) and probability between February and August in the historical period (*B*). Annual (*C*), February (*D*), and August (*E*) percent change in species richness, comparing future to historical periods (Future – Historical). Richness is defined as the number of species exceeding a probability of 0.2 and is expressed as a percentage of 87 retained taxa from the survey. The solid black contour indicates the region with greater than 10% new species occurring; the dashed black contour indicates the region with greater than 10% extirpated species (*Methods*).

strong MLD effect. The east–west asymmetry of MLD changes in the region (Fig. S1) contributes to projected longitudinal shifts. Increases in PAR in the northwest Atlantic (Fig. S1), driven by reductions in sea ice, have the potential to change the community in these regions where phytoplankton growth is often light-limited. Cloud-related changes in PAR over the subtropical North Atlantic, although of contrasting signs (Fig. S1), also appear to play an influential role. Increasing SST is important at lower latitudes and in the northwest Atlantic but exerts weaker influence in pelagic seas in higher latitudes where large MLD and PAR changes were dominant. The large breadth of temperature tolerance for many phytoplankton species (9, 13), particularly outside of the tropics, relative to the magnitude of projected temperature changes may account for this insensitivity.

The modeled climate responses of species, and consequently the estimated level of shift and shuffle projected for the North Atlantic, are uncertain for several reasons. First, we have examined a subset of all possible environmental and biological predictor variables, excluding potentially important environmental drivers such as the availability of iron and ocean acidification. Even though iron is relatively abundant in North Atlantic surface waters, it can limit phytoplankton growth in summer at higher latitudes and plays a role in shaping phytoplankton communities (37). However, we did not include iron in the SDM because the provision and biogeochemical cycling of iron in the surface ocean in the coming century, and consequently its ecological roles, remain highly uncertain (38). In the

case of ocean acidification, the large and widespread reductions in North Atlantic surface water pH projected in the coming century (1) have the potential to influence the growth and survival of many phytoplankton species (39). The future changes in pH are large in comparison with the seasonal and regional ranges in pH (40) in the historic period that would be used to construct SDMs. This limited pH overlap between historic and future periods restricts the utility of the bioclimate envelope approach for studying the effects of changing pH, and we therefore do not consider ocean acidification in this study.

We have also assumed that the realized niche for each taxon will not adjust as the climate changes, neglecting evolutionary change. However, the optimum temperature for growth and pH sensitivity for microbes evolves in response to changing conditions (41). Although the adaptive capacity of each phytoplankton for a range of stressors remains unknown, it is likely that phytoplankton microevolution will affect changes in species ranges (27). Similarly, the SDMs do not explicitly include the abundances of phytoplankton predators, and we do not consider how changing predator–prey interactions in the future may alter species distributions. Changing temperatures may differentially affect the growth rates and coupling of phytoplankton and their predators (42), and trophic mismatches disrupting the phenology of plankton appear likely (43). Each of these sources of uncertainty may potentially affect our results and should be investigated carefully in future studies, yet our projections are useful for estimating the potential change in marine phytoplankton

Fig. 4. Response of phytoplankton community to climate changes in the seven individual environmental factors considered, ranked in order of overall relative importance: (*A*) MLD, (*B*) PAR, (*C*) nitrate, (*D*) SST, (*E*) SSS, (*F*) phosphate, and (*G*) silicate. Values greater (less than) than 1/7 imply the driver is relatively important (unimportant) compared with the other drivers. The rankings are assigned by ordering the basin-averaged responses.

communities and can be compared with projections made with other numerical (1, 2, 10, 39) and statistical models (8, 9), as well as estimates of range shifts gleaned from terrestrial and marine historical data (36, 44).

Anthropogenic climate change over the coming century may drive North Atlantic phytoplankton species ranges and communities to move in space, or shift, and cause communities to internally reassemble, or shuffle. The projected poleward range shifts in this region are larger than previously estimated (36, 44) and may also be accompanied by significant and previously unanticipated longitudinal shifts. When integrated over a century of climate change, these range shifts are similar in size to large marine ecosystems and state exclusive economic zones, suggesting that the projected changes in the phytoplankton community may be of consequence to management of living marine resources (45). Although temperature has in the past been the focus of numerous studies on how anthropogenic climate affects marine ecosystems (9, 46, 47), the profound ecological changes in North Atlantic phytoplankton communities are driven not just by temperature but by dynamic regional changes in ocean circulation and surface conditions that imprint on mixed layer depth, light, salinity, and macronutrients. Thus, we suggest that future studies consider the effect of multiple environmental drivers acting in concert (48), rather than only temperature.

Methods

Species Distribution Models and Validation. Following on Irwin et al. (13), we diagnosed the SDM for each diatom and dinoflagellate in the CPR survey with the MaxEnt modeling method (14–17), which estimates the probability a species is present under any of the observed combinations of environmental conditions. MaxEnt is one of many approaches to species distribution modeling but is particularly well suited to using presence-only CPR data (49). It has been found to perform relatively well compared with other methods in modeling species distributions, particularly for species with small sample sizes (49, 50), and is well vetted and generally accepted by ecologists. For the MaxEnt analysis, we used software version 3.3.3k (www.cs.princeton.edu/~schapire/maxent/) and turned off threshold features in the response functions but allowed linear, quadratic, product, and hinge features. We performed 100 bootstrap resampling runs for each species (observation-based model and projections) and report the mean logistic probability and AUC score for each species (Table S1). As our study considered a large and diverse number of species, we used the default settings for all other tunable parameters in the MaxEnt software (15). We constructed the SDM for all CPR diatom and dinoflagellate taxa identified to species or genus level (~200 taxa), and present results only for the most robustly modeled 87 taxa that have minimum of 15 observations and an AUC score of 0.7 (SI Text). We have experimented extensively with the minimum observation number and AUC thresholds and find the models results are not overly sensitive to these choices.

For each SDM, we used training data from the CPR (SI Text) and climatological observational data describing seven key environmental parameters, averaged over the same standard survey areas: SST [World Ocean Atlas (WOA) 2009; https://www.nodc.noaa.gov/OC5/WOA09/pr_woa09.html] (51); SSS (WOA 2009) (52); MLD (the depth at which the potential density increases by 0.03 kg·m^{-3} from the surface; from the de Boyer Montégut climatology; www.ifremer.fr/cerweb/deboyer/mld/) (53); PAR at the ocean surface, calculated from the surface radiation budget (SRB); gewex-srb.larc.nasa.gov); surface nitrate concentration (WOA 2009) (54); surface phosphate concentration (WOA 2009) (54); and surface silicate concentration (WOA 2009) (54). For MLD, we used the inverse of MLD to lessen the importance of excessively deep MLDs at high latitudes. To estimate PAR, we multiplied the net incoming shortwave radiation (incoming shortwave minus outgoing shortwave) by a standard conversion factor of 0.46 (55). The SRB net shortwave data are comparable to output from the ESM2G model, which outputs the net downward shortwave flux at the seawater surface. We used time-varying CPR but climatological environmental data because quality time-varying data are not available for each environmental driver. This discrepancy may cause some blurring of the modeled phytoplankton niches.

Once the SDM for each species was constructed from observations, we calculated the logistic probability of occurrence, from 0 to 1, for each location, month of the year, and species in the model historical (1951–2000) and future (2051–2100) periods, using ESM2G model variables corresponding to the SDM predictor variables. Unlike the training data, the model data have 1° horizontal resolution. Our approach maps species biogeographies in historical and future climate states and allows for internally consistent projections of biogeographic change.

We also sought to assess the importance of climate-driven changes in each environmental driver to future phytoplankton biogeographies and communities (Fig. 4). To do so, we recalculated SDMs for each taxa using historical data for all drivers except for driver k, for which instead we used future data. The response in the phytoplankton community to the climate changes in the kth driver, Δ_k, was defined as the absolute difference in probability (P) between future and historical periods, summed over all months (j) and species (i):

$$\Delta_k = \sum_j \sum_i \left| P_{i,j}^{\text{Future for }k\text{th driver only}} - P_{i,j}^{\text{Historical}} \right|.$$

We normalized Δ_k by the sum of the responses across all seven variables, such that a value greater (less than) than 1/7 implies that change in a given driver has a relatively large (small) effect.

Species Core Range, Core Range Central Position, and Range Shifts. The core range is defined as the geographic area with logistic probabilities greater than 50% of the maximum logistic probability of presence for each species. The focus on core range, defined by species-specific but proportional levels of logistic probability, identifies periods and places where a given taxa is most likely to occur and enables diagnosis of how this range may shift through time. The core range is a relatively narrow description of total species range and acknowledges that the high population sizes and dispersal rates of marine microbes may lead to their being present outside their realized niche (56). Previous studies have found that changes in range central position through time tend to be less dynamic than for range leading edges (36).

The core range central position of each species for each month of the year is calculated by taking the average of all latitude and longitude points within the core range, weighted by the probability of occurrence and grid cell area (km^2; the area of grid cells decreases toward to pole). The climate-mediated range shifts for each month of the year are calculated by subtracting the core range central position in 1951–2000 from the core range central position in 2051–2100. We report the annual median range shift (Fig. 2 and in text) and convert to units of km·dec^{-1}. The interquartile range bounds given indicate the range of species responses projected, not uncertainty regarding the climate or species distribution models. The range shifts reported in the text and presented in Fig. 2 are qualitatively similar over a range of percentage cutoff values (40–60%) used to define the core range. Similarly, if instead we define the core range as location with a relatively high fixed probability cutoff (in this case, greater than 0.2), the results in Fig. 2 are broadly conserved.

Bray–Curtis Similarity Index and Community Change. We estimated the similarity between any two phytoplankton communities, community A and community B, with the Bray–Curtis similarity index, or S (57):

$$S = 1 - \frac{\Sigma_i \left| P_i^A - P_i^B \right|}{\Sigma_i \left| P_i^A + P_i^B \right|},$$

where P_i^A and P_i^B are the probabilities of species i occurring in communities A and B, respectively. In Fig. 2C, we calculated S at each point on the map by comparing the historical probabilities at a typical subpolar location (P_i^A) with historical probabilities in each one of the surrounding points (P_i^B). In Fig. 2E, we used historical probabilities at a typical reference point in the subtropical gyre instead. Unsurprisingly, in both cases, S generally decreases with increasing distance from the reference location. Fig. 2 D and F show a similar calculation, but we instead compared the historical community at the reference location to projected future communities at each point in the domain. This calculation shows that communities move in space relative to their initial positions in the historical period. The two reference locations in Fig. 2 were selected to reflect communities characteristic of the subtropical and subpolar ocean gyres. In Fig. 3 A and B, we calculated S on a point-by-point basis, comparing annual median future and historical probabilities (Fig. 3A) and February and August probabilities in the historical period (Fig. 3B). We report the percentage change in community structure as $100(1 - S)$.

We also estimated new and extirpated species. New species are species that historically had low probabilities ($Pr^{\text{Historical}} < 0.2$) and significantly increase in the future ($Pr^{\text{Future}} - Pr^{\text{Historical}} > 0.2$); extirpated species are species that historically had high probabilities ($Pr^{\text{Historical}} > 0.2$) and significantly decrease in the future ($Pr^{\text{Future}} - Pr^{\text{Historical}} < -0.2$).

ECOLOGY

ENVIRONMENTAL SCIENCES

1. Bopp L, et al. (2013) Multiple stressors of ocean ecosystems in the 21st century: Projections with CMIP5 models. *Biogeosciences* 10(10):6225–6245.
2. Steinacher M, et al. (2010) Projected 21st century decrease in marine productivity: A multi-model analysis. *Biogeosciences* 7(3):979–1005.
3. Capotondi A, et al. (2012) Enhanced upper ocean stratification with climate change in the CMIP3 models. *J Geophys Res* 117(C4):2156–2202.
4. Manabe S, Stouffer RJ (1993) Century-scale effects of increased atmospheric CO2 on the ocean-atmosphere system. *Nature* 364(6434):215–218.
5. Delworth TL, Manabe S, Stouffer RJ (1993) Interdecadal variations of the thermohaline circulation in a coupled ocean-atmosphere model. *J Clim* 6(11):1993–2011.
6. Stock CA, Dunne JP, John JG (2014) Drivers of trophic amplification of ocean productivity trends in a changing climate. *Biogeosciences* 11(7):11331–11359.
7. Doney SC, et al. (2012) Climate change impacts on marine ecosystems. *Annu Rev Mar Sci* 4(1):11–37.
8. Flombaum P, et al. (2013) Present and future global distributions of the marine Cyanobacteria *Prochlorococcus* and *Synechococcus*. *Proc Natl Acad Sci USA* 110(24):9824–9829.
9. Thomas MK, Kremer CT, Klausmeier CA, Litchman E (2012) A global pattern of thermal adaptation in marine phytoplankton. *Science* 338(6110):1085–1088.
10. Dutkiewicz S, Scott JR, Follows MJ (2013) Winners and losers: Ecological and biogeochemical changes in a warming ocean. *Glob Biogeochem Cycles* 27(2):463–477.
11. Finkel ZV, et al. (2010) Phytoplankton in a changing world: Cell size and elemental stoichiometry. *J Plankton Res* 32(1):119–137.
12. Pearson RG, Dawson T (2003) Predicting the impacts of climate change on the distribution of species: Are bioclimate envelope models useful? *Glob Ecol Biogeogr* 12(5):361–371.
13. Irwin AJ, Nelles AM, Finkel ZV (2012) Phytoplankton niches estimated from field data. *Limnol Oceanogr* 57(3):787–797.
14. Merow C, Smith MJ, Silander JA (2013) A practical guide to MaxEnt for modeling species' distributions: What it does, and why inputs and settings matter. *Ecography* 36(10):1058–1069.
15. Phillips SJ, Dudík M (2008) Modeling of species distributions with Maxent: New extensions and comprehensive evaluation. *Ecography* 31(2):161–175.
16. Elith J, et al. (2011) A statistical explanation of MaxEnt for ecologists. *Divers Distrib* 17(1):43–57.
17. Phillips SJ, Anderson RP, Schapire RE (2006) Maximum entropy modeling of species geographic distributions. *Ecol Modell* 190(3-4):231–259.
18. Richardson AJ, et al. (2006) Using continuous plankton recorder data. *Prog Oceanogr* 68(1):27–74.
19. Barton AD, et al. (2013) On the roles of cell size and trophic strategy in North Atlantic diatom and dinoflagellate communities. *Limnol Oceanogr* 58(1):254–266.
20. Dunne JP, et al. (2013) GFDL's ESM2 Global Coupled Climate–Carbon Earth System Models. Part I: Physical formulation and baseline simulation characteristics. *J Clim* 25(19):6646–6665.
21. Dunne JP, et al. (2013) GFDL's ESM2 Global Coupled Climate–Carbon Earth System Models. Part II: Carbon system formulation and baseline simulation characteristics. *J Clim* 26(7):2247–2267.
22. Brun P, et al. (2015) Ecological niches of open ocean phytoplankton taxa. *Limnol Oceanogr* 60(3):1020–1038.
23. Cushing DH (1989) A difference in structure between ecosystems in strongly stratified waters and in those that are weakly stratified. *J Plankton Res* 11(1):1–13.
24. Taylor AH, et al. (1993) Seasonal succession in the pelagic ecosystem of the North Atlantic and the utilization of nitrogen. *J Plankton Res* 15(8):875–891.
25. Henson S, Lampitt R, Johns D (2012) Variability in phytoplankton community structure in response to the North Atlantic Oscillation and implications for organic carbon flux. *Limnol Oceanogr* 57(6):1591–1601.
26. Rivero-Calle S, et al. (2015) Multidecadal increase in North Atlantic coccolithophores and the potential role of rising CO2. *Science* 350(6267):1533–1537.
27. Irwin AJ, Finkel ZV, Müller-Karger FE, Troccoli Ghinaglia L (2015) Phytoplankton adapt to changing ocean environments. *Proc Natl Acad Sci USA* 112(18):5762–5766.
28. Barnard RT, et al. (2004) Continuous plankton records: Plankton atlas of the North Atlantic Ocean (1958-1999). II. Biogeographical charts. *Mar Ecol Prog Ser* (Suppl):11–75.
29. Barton AD, et al. (2013) The biogeography of marine plankton traits. *Ecol Lett* 16(4):522–534.
30. Marinov I, et al. (2013) North-south asymmetry in the modeled phytoplankton community response to climate change over the 21st century. *Glob Biogeochem Cycles* 27(4):1274–1290.
31. Margalef R (1978) Life-forms of phytoplankton as survival alternatives in an unstable environment. *Oceanol Acta* 1(4):493–509.
32. Barton AD, Lozier MS, Williams RG (2015) Physical controls of variability in North Atlantic phytoplankton communities. *Limnol Oceanogr* 60(1):181–197.
33. Bopp L, et al. (2005) Response of diatoms distribution to global warming and potential implications: A global model study. *Geophys Res Lett* 32(19):L19606.
34. Hansen B, Bjørnsen BW, Hansen PJ (1997) Zooplankton grazing and growth: Scaling within the 2-2000um body size range. *Limnol Oceanogr* 42(4):687–704.
35. Edwards KF, Thomas MK, Klausmeier CA, Litchman E (2012) Allometric scaling and taxonomic variation in nutrient utilization traits and maximum growth rate of phytoplankton. *Limnol Oceanogr* 57(2):554–566.
36. Poloczanska ES, et al. (2013) Global imprint of climate change on marine life. *Nat Clim Change* 3(10):919–925.
37. Moore CM, et al. (2013) Processes and patterns of oceanic nutrient limitation. *Nat Geosci* 6(9):701–710.
38. Boyd PW, Ellwood MJ (2010) The biogeochemical cycle of iron in the ocean. *Nat Geosci* 3(10):675–682.
39. Dutkiewicz S, et al. (2015) Impact of ocean acidification on the structure of future phytoplankton communities. *Nature Clim Change* 5(11):1002–1006.
40. Takahashi T, et al. (2014) Climatological distributions of pH, pCO2, total CO2, alkalinity, and CaCO3 saturation in the global surface ocean, and temporal changes at selected locations. *Mar Chem* 164:95–125.
41. Collins S, Rost B, Rynearson TA (2014) Evolutionary potential of marine phytoplankton under ocean acidification. *Evol Appl* 7(1):140–155.
42. Rose JM, Caron DA (2007) Does low temperature constrain the growth rates of heterotrophic protists? Evidence and implications for algal blooms in cold waters. *Limnol Oceanogr* 52(2):886–895.
43. Edwards M, Richardson AJ (2004) Impact of climate change on marine pelagic phenology and trophic mismatch. *Nature* 430(7002):881–884.
44. Parmesan C, Yohe G (2003) A globally coherent fingerprint of climate change impacts across natural systems. *Nature* 421(6918):37–42.
45. Stock CA, et al. (2011) On the use of IPCC-class models to assess the impact of climate on Living Marine Resources. *Prog Oceanogr* 88(1-4):1–27.
46. Pinsky ML, Worm B, Fogarty MJ, Sarmiento JL, Levin SA (2013) Marine taxa track local climate velocities. *Science* 341(6151):1239–1242.
47. Burrows MT, et al. (2011) The pace of shifting climate in marine and terrestrial ecosystems. *Science* 334(6056):652–655.
48. Boyd PW, Hutchins DA (2012) Understanding the responses of ocean biota to a complex matrix of cumulative anthropogenic change. *Mar Ecol Prog Ser* 470:125–135.
49. Elith J, et al. (2006) Novel methods improve prediction of species' distributions from occurrence data. *Ecography* 29(2):129–151.
50. Wisz MS, et al. (2008) Effects of sample size on the performance of species distribution models. *Divers Distrib* 14(5):763–773.
51. Locarnini RA, et al. (2010) *Temperature*, World Ocean Atlas 2009, NOAA Atlas NESDIS, ed Levitus S (US Government Printing Office, Washington, DC), Vol 1.
52. Antonov JI, et al. (2010) *Salinity*, World Ocean Atlas 2009, NOAA Atlas NESDIS, ed Levitus S (US Government Printing Office, Washington, DC), Vol 2.
53. de Boyer Montégut C, et al. (2004) Mixed layer depth over the global ocean: An examination of profile data and a profile-based climatology. *J Geophys Res* 109(C12):C12003.
54. Garcia HE, et al. (2010) *Nutrients (Phosphate, Nitrate, Silicate)*, World Ocean Atlas 2009, NOAA Atlas NESDIS, ed Levitus S (US Government Printing Office, Washington, DC), Vol 4.
55. Baker KS, Frouin R (1987) Relation between photosynthetically available radiation and total insolation at the ocean surface under clear skies. *Limnol Oceanogr* 32(6):1370–1377.
56. Leibold MA, et al. (2004) The metacommunity concept: A framework for multi-scale community ecology. *Ecol Lett* 7(7):601–613.
57. Somerfield PJ (2008) Identification of the Bray-Curtis similarity index: Comment on Yoshioka (2008). *Mar Ecol Prog Ser* 372:303–306.
58. Hirata T, et al. (2011) Synoptic relationships between surface chlorophyll-a and diagnostic pigments specific to phytoplankton functional types. *Biogeosciences* 8(2):311–327.
59. Barton AD, Greene CH, Monger BC, Pershing AJ (2003) The Continuous Plankton Recorder survey and the North Atlantic Oscillation: Interannual- to Multidecadal-scale patterns of phytoplankton variability in the North Atlantic Ocean. *Prog Oceanogr* 58(2-4):337–358.
60. Lévy M, Jahn O, Dutkiewicz S, Follows MJ (2014) Phytoplankton diversity and community structure affected by oceanic dispersal and mesoscale turbulence. *Limnol Oceanogr Fluids Environ* 4(1):67–84.
61. Gnanadesikan A, Dunne JP, Msadek R (2014) Connecting Atlantic temperature variability and biological cycling in two earth system models. *J Mar Syst* 133:39–54.
62. Deser C, Phillips AS, Alexander MA (2010) Twentieth century tropical sea surface temperature trends revisited. *Geophys Res Lett* 37(10):L10701.
63. Rahmstorf S, et al. (2015) Exception twentieth-century slowdown in Atlantic Ocean overturning circulation. *Nat Clim Change* 5(5):475–480.
64. Stroeve JC, et al. (2012) Trends in Arctic sea ice extent from CMIP5, CMIP3 and observations. *Geophys Res Lett* 39(16):L16502.
65. Phillips SJ, et al. (2009) Sample selection bias and presence-only distribution models: Implications for background and pseudo-absence data. *Ecol Appl* 19(1):181–197.
66. Lobo JM, Jiménez-Valverde A, Real R (2008) AUC: a misleading measure of the performance of predictive distribution models. *Glob Ecol Biogeogr* 17(2):145–151.
67. Yackulic CB, et al. (2013) Presence-only modelling using MAXENT: When can we trust the inferences? *Methods Ecol Evol* 4(3):236–243.